Synthesis, microstructure and magnetic properties of Heusler Co_2FeSn nanoparticles

Tao Li, Jihong Duan, Chunkui Yang, Xinli Kou

Key Laboratory for Magnetism and Magnetic Materials of the Ministry of Education, School of Physical Science and Technology, Lanzhou University, Lanzhou 730000, People's Republic of China
E-mail: kouxl@lzu.edu.cn

Published in Micro & Nano Letters; Received on 25th November 2012; Revised on 19th January 2013; Accepted on 1st February 2013

Heusler Co_2FeSn nanoparticles in a *B*2-type cubic structure were synthesised for the first time using a simple solution reduction method. X-ray diffraction, a scanning electron microscope, an energy dispersive spectrometer and a vibrating sample magnetometer were used to characterise the synthesised products. The crystal structure and composition of the samples vary with the concentration of potassium hydroxide, synthesis temperature and reaction time. Magnetic measurement reveals that the obtained Co_2FeSn nanoparticles are soft magnetic at room temperature. The Co_2FeSn nanoparticles synthesised in this work are magnetically superior and economically feasible for spintronic applications.

1. Introduction: The Co_2YZ (Y = transition metals, Z = main group element) Heusler compounds are of special interest for applications as they exhibit a large saturation magnetisation and high values of Curie temperatures. They are a remarkable class of magnetic materials that hold the greatest potential to achieve half-metallicity at room temperature and are also ideal for spintronics [1, 2]. Up to now, a large number of Co_2YZ compounds have been synthesised and their structures and physical properties have been investigated [3], however new properties and potential fields of applications still emerge constantly.

As we know, magnetic nanoparticles have gained enormous interest for applications in various fields such as data storage devices, catalysis, drug delivery and biomedical imaging [4–6]. Nanoscale magnetic particles demonstrate many novel physical and chemical properties mainly attributed to their small size and high surface to volume ratio. Since the nanocrystal materials exhibit structure and physical properties that are quite different from their bulk counterparts, a breakthrough from the viewpoint of materials design is the synthesis of nanoparticles of Heusler compounds [7]. The investigation of Co_2YZ nanoparticles would open new directions for spintronic applications. However, up to now, there are very few studies on the synthesis of Co_2YZ nanoparticles. It is only recently that Co_2FeGa nanoparticles were successfully synthesised by a wet impregnation method and their magnetic and structural properties were investigated [8]. Co_2FeGa nanoparticles were found to exhibit the ordered $L2_1$ structure with a slightly reduced lattice parameter compared with the bulk material. The Co_2FeGa nanoparticles are soft magnetic but slightly harder compared with polycrystalline bulk material [8]. Ni_2MnGa nanoparticles with different crystallite size and crystal structure were prepared by the ball-milling method combined with a post-annealing process by Wang *et al.* [9]. The ferromagnetic Ni_2MnGa nanoparticles undergo various sequences of structural phase transitions that are tailored by the crystallite size, atomic order and intrinsic magnetic structure [9]. It was found that these two kinds of Co_2YZ nanoparticles have new structures and new magnetic properties, which are completely different from their coarse-grained counterparts.

Co_2FeSn is a cheap Heusler alloy and is predicted to have considerably large magnetic moment according to Slater-Pauling behaviour [10, 11]. To our knowledge, Co_2FeSn nanoparticles have never been synthesised before. In X_2YZ Heusler compounds crystallised in the cubic $L2_1$ ordered structure, the X atoms occupy the Wyckoff position 8*c* (1/4, 1/4, 1/4), the Y and the Z atoms are located at 4*a* (0, 0, 0) and 4*b* (1/2, 1/2, 1/2), respectively. Depending on site exchangeability, various types of site disorders have been identified. Complete disorder in X_2YZ occurs when all sites are equivalent, resulting in the *A*2-type disorder [body-centred cubic (bcc) lattice]. If only the Y and Z atoms are exchangeable, the 4*a* and 4*b* positions become equivalent, leading to a *B*2 ordered structure (simple cubic lattice) [3]. In our present work, Co_2FeSn nanoparticles in the *B*2-type cubic structure have been obtained using the solution reduction method. The influence of synthesis temperature, concentration of potassium hydroxide (KOH) solution and reaction time on the crystal structure and composition of the samples have been studied. The relationship between the microstructure and magnetic properties of the samples are discussed.

2. Experimental: All chemical reagents were of analytical grade and used as received without further purification. Firstly, 0.476 g cobalt chloride ($CoCl_2{\cdot}6H_2O$), 0.278 g ferrous sulphate ($FeSO_4{\cdot}7H_2O$) and 0.226 g stannous chloride ($SnCl_2{\cdot}2H_2O$) were dissolved in 10 ml water to obtain a mixed solution (solution 1). $NaH_2PO_2{\cdot}H_2O$ solution (10.599 g in 5 ml water) was added drop-wise to 10 ml KOH solution (solution 2). Then, with solution 2 being vigorously stirred under bubbling Ar, solution 1 was added drop-wise to solution 2. After the dripping process was completed, the reaction was carried out under vigorous stirring at various temperatures (25–55°C) for 5–150 h. Ar bubbling was maintained during the experiment. Finally, the solution was centrifuged at 10 000 rpm for 5 min. The collected particles were washed several times with deionised water and ethanol, magnetically separated and allowed to dry at room temperature.

The crystal structures of the samples were analysed by X-ray diffraction (XRD) on a Rigaku D/max-2400 diffractometer with Cu K_α radiation ($\lambda = 1.54056$ Å). The morphology of the samples was observed on a HITACHI S-4800 scanning electron microscope (SEM). For SEM observation, the powder was first dispersed in ethanol and dripped onto a piece of wafer, then baked at 50°C for several hours. Sample composition was measured by the energy dispersive spectrometer (EDS). The magnetic properties of the samples were studied by a Lake Shore 7304 vibrating sample magnetometer at room temperature.

3. Results and discussion

3.1. Synthesis and structure: For the preparation of metal and alloy nanoparticles, the solution reduction method has many advantages as compared with other methods since it is a simple and low-cost method and can yield new and metastable structures not accessible using traditional methods [12, 13]. In theory, the reduction of any metal with a standard electrode potential ($E°$) more positive than −0.481 V, should be possible at room temperature, given a sufficient excess of reducing agent and proper control of pH [14]. Considering the $E°$ value of Co^{2+}/Co,

Table 1 Main experimental parameters for synthesis

Sample no.	KOH concentration, M	Synthesis temperature, °C	Reaction time, h	Composition ratio Co:Fe:Sn	Saturation magnetisation M_S, emu/g	Coercivity H_C, Oe
1	25	25	150	2.0:1.06:0.21	141	68
2	20	25	150	2.0:1.05:0.18	132	143
3	15	40	150	2.0:1.00:0.33	118	74
4	15	55	150	2.0:1.16:0.47	92	68
5	15	25	5	–		
6	15	25	60	–		
7	15	25	100	2.0:0.92:0.56		
8	15	25	150	2.0:1.02:0.93	82	40

The composition ratio Co:Fe:Sn, saturation magnetisation and coercivity of the samples.

Fe^{2+}/Fe and Sn^{2+}/Sn are −0.28, −0.447 and −0.14 V, respectively, we used a solution reduction method for the preparation of Co_2FeSn nanoparticles in our present work. The synthesis was performed in aqueous solution using inexpensive metallic salt resources and sodium hypophosphite ($NaH_2PO_2{\cdot}H_2O$) as reducing agent. Various concentrations of KOH solution, synthesis temperatures and reaction time were used to synthesise Co_2FeSn nanoparticles. The main parameters for synthesis are shown in Table 1. The average elemental composition of the samples determined by EDS is also shown in Table 1. Fig. 1 shows the XRD patterns of the samples synthesised at different experimental conditions as shown in Table 1.

Fig. 1*a* shows the XRD patterns of the samples prepared using different concentrations of KOH, namely 25, 20 and 15 M labelled as samples 1, 2 and 8, respectively. For the samples prepared with 25 and 20 M KOH, the XRD patterns indicate the presence of characteristic reflections of the bcc structure. The prominent diffraction peaks at about $2\theta = 43.8°$, 64.1° and 81.0° corresponded to scattering from (110), (200) and (211) crystal planes, respectively. For the sample prepared using 15 M KOH solution (sample 8), the superlattice reflection (100) at $2\theta = 30.4°$ is present which indicates the *B*2 ordered structure [15]. The diffraction pattern of sample 8 was consistent with the theoretical XRD pattern of Co_2FeSn, which was simulated under the assumption of a *B*2 ordered structure (Fig. 1*d*). Our results indicate that with the increase of KOH concentrations, the structure of the products changed from *B*2-type ordered structure to bcc disordered structure. With the increase of KOH concentrations, the reaction kinetics increases [16], this will be of benefit for the formation of the disordered structure. Meanwhile, the major diffraction peak (110) of sample 8 shifted obviously towards the left compared with samples 1 and 2, which indicates the increased lattice constant of sample 8. According to the EDS results in Table 1, the composition ratios of Co:Fe:Sn are 2.0:1.06:0.21 and 2.0:1.05:0.18 for samples 1 and 2, respectively. For sample 8, the composition ratio of Co:Fe:Sn is 2.0:1.02:0.93, which is within experimental error of the nominal 2:1:1 composition of Co_2FeSn. As the content of the Sn atom in sample 8 is more than those in samples 1 and 2, the lattice dilatation is reasonable since the radius of the Sn atom is larger than that of Fe and Co.

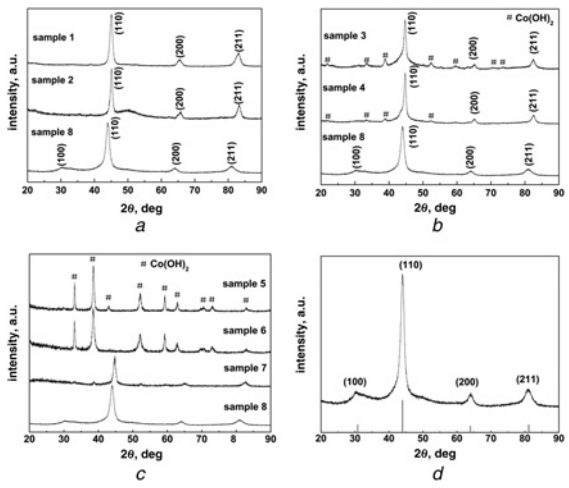

Figure 1 *XRD patterns*
a Samples 1, 2 and 8
b Samples 3, 4 and 8
c Samples 5, 6, 7 and 8
d Sample 8, tick marks below the pattern show the positions of the allowed Bragg reflection and the relative intensities of the reflections for Co_2FeSn, which were simulated under the assumption of *B*2-ordered structure

Fig. 1*b* shows the XRD patterns of the samples synthesised at different temperatures. For the sample prepared at room temperature (sample 8), the XRD data indicates a *B*2-type cubic structure of the prepared Co_2FeSn nanoparticles as described before. When the synthesis temperature was increased to 40°C (sample 3) and 55°C (sample 4), besides the characteristic diffraction peaks (110), (200) and (211) of the bcc structure, several weak diffraction peaks occur, as marked by '#', and were assigned to a small amount of $Co(OH)_2$ in the sample. It indicated that the increased synthesis temperature led to the appearance of $Co(OH)_2$ in the sample. Although the increased synthesis temperature can accelerate the reaction rate, however, the solution becomes unstable at higher temperature, where cobalt hydroxides will precipitate during the process [17].

Fig. 1*c* shows the XRD patterns of the samples synthesised using different reaction times at room temperature using 15 M KOH solution. When the reaction time is 5 and 60 h (samples 5 and 6), the main phase is $Co(OH)_2$. When the reaction time was increased to 100 h (sample 7), the diffraction peaks of $Co(OH)_2$ nearly disappeared. The main diffraction peaks of the bcc structure appear at $2\theta = 44.3°$. When the reaction time was increased to 150 h (sample 8), the superlattice reflection (100) at $2\theta = 30.4°$ is present which indicates the *B*2 ordered structure of the prepared Co_2FeSn nanoparticles as described before. With the increase of the reaction time, the atoms may have enough time to enter the specific structure position, this is beneficial to the formation of the ordered *B*2 structure. Besides, the major diffraction peak (110) of sample 8 shifted obviously towards the left which indicates the increased lattice constant as compared with sample 7. From Table 1 we can see that when the reaction time was increased from 100 to 150 h, the composition ratio of Co:Fe:Sn changed from 2.0:0.92:0.56 to 2.0:1.02:0.93. The content of Sn atoms in the sample increased with increasing reaction time. As the content of Sn atoms in sample 8 is more than those in sample 7, the lattice constant of sample 8 increases since the radius of the Sn atom is larger than that of Fe and Co.

Hence, our results show that the synthesis temperature, concentration of KOH solution and reaction time are the key parameters determining the structure and composition of the final products. *B*2-type cubic Co_2FeSn nanoparticles with nominal 2:1:1

doi: 10.1049/mnl.2012.0905

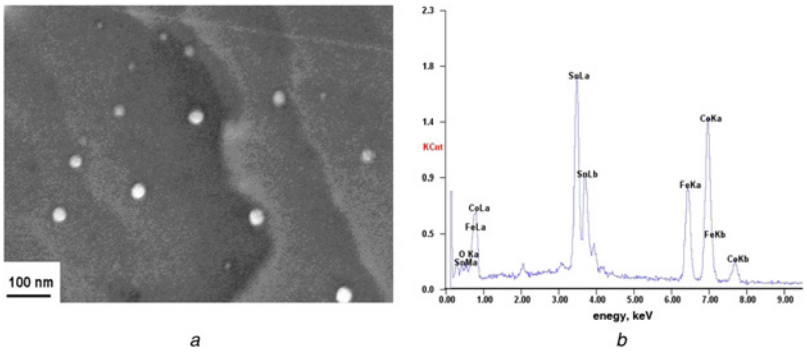

Figure 2 *SEM micrograph and EDS result of sample 8*
a SEM micrograph
b EDS result of sample 8

composition (sample 8) can be obtained at 25°C by the solution reduction method, using a 15 M KOH solution and a reaction time of 150 h. Fig. 2 shows the SEM image and EDS result of sample 8. The particles are nearly spherical and are well dispersed. The particle size is in the range of 20–40 nm.

The possible reaction process for the synthesis of Co_2FeSn nanoparticles can be described as follows [17, 18]:

$$Co^{2+} + H_2PO_2^- + 3OH^- \rightarrow Co + HPO_3^{2-} + 2H_2O \quad (1)$$

$$Fe^{2+} + H_2PO_2^- + 3OH^- \rightarrow Fe + HPO_3^{2-} + 2H_2O \quad (2)$$

$$Sn^{2+} + H_2PO_2^- + 3OH^- \rightarrow Sn + HPO_3^{2-} + 2H_2O \quad (3)$$

$$2Co + Fe + Sn \rightarrow Co_2FeSn \quad (4)$$

$$3H_2PO_2^- \rightarrow H_2PO_3^- + H_2O + 2OH^- + 2P \quad (5)$$

$$H_2PO_2^- + H_2O \rightarrow H_2PO_3^- + H_2 \quad (6)$$

At the start of the experiment, Co^{2+}, Fe^{2+} and Sn^{2+} were reduced to Co, Fe and Sn atoms by reducing agent $NaH_2PO_2{\cdot}H_2O$, according to reactions (1)–(3), respectively. Then, the active Co, Fe and Sn atoms will react with each other and Co_2FeSn is formed. From the above chemical reactions (1)–(3), KOH is found to play a major role in reducing metal ion to metal atom. The OH^- helps in adjusting the reduction potential of the species as well as controlling the reaction rate [19, 20], which results in the co-reduction of Co^{2+}, Fe^{2+} and Sn^{2+} while Co_2FeSn were synthesised in situ. From the above chemical reactions (5) and (6), it can be seen that hydrogen and phosphorus are the by-products. Hydrogen forms bubbles and leaves the solution during the reaction, phosphorus is washed away.

3.2. Magnetic properties: Fig. 3 shows the magnetic hysteresis loops of samples 1, 2, 3, 4 and 8 measured at room temperature, from which the magnetic parameters such as saturation magnetisation (M_S) and coercivity (H_C) are determined, and the

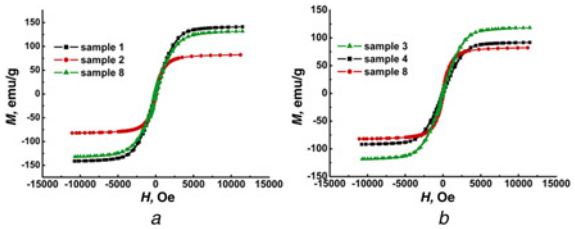

Figure 3 *Magnetic hysteresis loops of*
a Samples 1, 2 and 8
b Samples 3, 4 and 8

results are listed in Table 1. It can be seen from Fig. 3 that all the samples are ferromagnetic at room temperature. From Table 1 we can see that the M_S of sample 8 is lower than those of samples 1 and 2. It is considered that the magnetic properties of the samples are affected by the chemical composition and crystal structure of the sample. According to the EDS results in Table 1, the large content of non-magnetic Sn in sample 8 caused decreasing of M_S. Furthermore, the enlarged value of M_S of samples 1 and 2 can be attributed to disorder [21, 22]. As described in Section 3.1, XRD results have indicated the disordered *A*2 structure (bcc) of samples 1 and 2 and the ordered *B*2 cubic structure of sample 8. Wurmehl *et al.* [22] calculated the magnetic moments for different kinds of disorder of Co_2FeAl and reported that the increase of the magnetic moment in the disordered *A*2 structure emerges mainly from an increase of the magnetic moment of the Co atoms. From Table 1 we can also see that the M_S of sample 8 is lower than those of samples 3 and 4. Although the small amount of $Co(OH)_2$ in samples 3 and 4 would cause decreasing of M_S, the lower content of non-magnetic Sn and the disordered structure of samples 3 and 4 would lead to a larger value of M_S as discussed above.

As the stoichiometric Co_2FeSn nanoparticles with the *B*2-type cubic structure have never been synthesised before, we pay more attention to the magnetic properties of sample 8. From Table 1 we can see that the saturation magnetisation and the coercivity of sample 8 are 82 emu/g and 40 Oe, respectively. Accordingly, the magnetic moment per unit cell is calculated to be 4.31 μ_B, which is lower than the theoretically calculated value of 5.53 μ_B for the Co_2FeSn compound [11]. The value of M_S is comparable with most of bulk Co_2YZ Heusler compounds [23]. Compared with previous reports about the Heusler Co_2FeGa nanoparticles prepared by Basit *et al.* [8] which have a magnetic moment of 4.77 μ_B and H_C of 7.7 KA/m at room temperature, the values of M_S and H_C of the Co_2FeSn nanoparticles (sample 8) are smaller. Furthermore, the coercivity of sample 8 is lower than previous reports about the FeCo nanoparticles using the polyol process [24–26]. The low coercivity of the Co_2FeSn nanoparticles synthesised using the low-cost solution reduction method being reported in the present work, makes them viable for many applications in the engineering and technology industries.

4. Conclusions

Co_2FeSn nanoparticles in the *B*2-type cubic structure with nominal 2:1:1 composition can be obtained at 25°C by the solution reduction method, using a 15 M KOH solution and a reaction time of 150 h.

As the concentration of KOH is increased from 15 to 25 M, XRD results indicate phase transition from the *B*2-type cubic structure to the bcc structure, the content of Sn in the sample decreases, and the value of M_S increases.

As the synthesis temperature is increased from 25 to 55°C, phase transition from the *B*2-type cubic structure to a mixture of bcc and $Co(OH)_2$ phase is observed.

When the reaction time is decreased from 150 to 5 h, the phase structure of the sample obviously changes from the *B*2-type cubic structure to the bcc structure and then to $Co(OH)_2$, the content of Sn in the sample increases.

The obtained Heusler Co_2FeSn nanoparticles with the particle size of 20–40 nm are ferromagnetic at room temperature and have the M_S of 82 emu/g and H_C of 40 Oe. The Co_2FeSn nanoparticles synthesised using the low-cost solution reduction method in our work are magnetically superior and economically feasible for technological applications.

5. Acknowledgments: This work was supported by the National Natural Science Foundation of China (grant no. 51201082) and the Natural Science Foundation of Gansu Province (grant no. 1010RJZA088).

6 References

[1] Felser C., Fecher G.H., Balke B.: 'Spintronics: a challenge for materials science and solid-state chemistry', *Angew. Chem. Int. Ed.*, 2007, **46**, pp. 668–699

[2] Wurmehl S., Fecher G.H., Kandpal H.C., Ksenofontov V., Felser C., Lin H.J.: 'Investigation of Co_2FeSi: the Heusler compound with highest Curie temperature and magnetic moment', *Appl. Phys. Lett.*, 2006, **88**, pp. 032503–032505

[3] Graf T., Felser C., Parkin S.S.P.: 'Simple rules for the understanding of Heusler compounds', *Prog. Solid State Chem.*, 2011, **39**, pp. 1–50

[4] Sun S., Murray C.B., Weller D., Folks L., Moser A.: 'Monodisperse FePt nanoparticles and ferromagnetic FePt nanocrystal superlattices', *Science*, 2000, **287**, pp. 1989–1992

[5] Sun S.: 'Recent advances in chemical synthesis, self-assembly, and applications of FePt nanoparticles', *Adv. Mater.*, 2006, **18**, pp. 393–403

[6] Jun Y.W., Lee J.H., Cheon J.: 'Chemical design of nanoparticle probes for high-performance magnetic resonance imaging', *Angew. Chem. Int. Ed.*, 2008, **47**, pp. 5122–5135

[7] Felser C., Hillebrands B.: 'Cluster issue on Heusler compounds and devices', *J. Phys. D, Appl. Phys.*, 2009, **42**, pp. 080301–080302

[8] Basit L., Wang C.H., Jenkins C.A., Balke B., Ksenofontov V., Fecher G.H.: 'Heusler compounds as ternary intermetallic nanoparticles', *J. Phys. D, Appl. Phys.*, 2009, **42**, pp. 084018–084024

[9] Wang Y.D., Ren Y., Nie Z.H., *ET AL.*: 'Structural transition of ferromagnetic Ni_2MnGa nanoparticles', *J. Appl. Phys.*, 2007, **101**, pp. 063530–063535

[10] Özdoğan K., Aktaş B., Galanakis I., Şaşıoğlu E.: 'Influence of mixing the low-valent transition metal atoms (Y, Y*=Cr, Mn, Fe) on the properties of the quaternary $Co_2[Y_{1-x}Y^*_x]Z$ (Z=Al, Ga, Si, Ge, Sn) Heusler compounds', *J. Appl. Phys.*, 2007, **101**, pp. 073910–073918

[11] Gilleβen M., Dronskowski R.: 'A combinatorial study of full Heusler alloys by first-principles computational methods', *J. Comput. Chem.*, 2009, **30**, pp. 1290–1299

[12] Leonard B.M., Bhuvanesh N.S.P., Schaak R.E.: 'Low-temperature polyol synthesis of $AuCuSn_2$ and $AuNiSn_2$: using solution chemistry to access ternary intermetallic compounds as nanocrystals', *J. Am. Chem. Soc.*, 2005, **127**, pp. 7326–7327

[13] Zhao Y., Zhang Y., Zhu H., Hadjipanayis G.C., Xiao J.Q.: 'Low-temperature synthesis of hexagonal (wurtzite) ZnS nanocrystals', *J. Am. Chem. Soc.*, 2004, **126**, pp. 6874–6875

[14] Cushing B.L., Kolesnichenko V.L., O'Connor C.J.: 'Recent advances in the liquid-phase syntheses of inorganic nanoparticles', *Chem. Rev.*, 2004, **104**, pp. 3893–3946

[15] Graf T., Casper F., Winterlik J., Balke B., Fecher G.H., Felser C.: 'Crystal structure of new Heusler compounds', *Z. Anorg. Allg. Chem.*, 2009, **635**, pp. 976–981

[16] Zhang L., Wang H., Li J.: 'Solution reduction synthesis and characterizations of HCP Co nanoplatelets', *Mater. Chem. Phys.*, 2009, **116**, pp. 514–518

[17] Pang J., Li Q., Wang W., Xu X., Zhai J.: 'Preparation and characterization of electroless Ni–Co–P ternary alloy on fly ash cenospheres', *Surf. Coat. Technol.*, 2011, **205**, pp. 4237–4242

[18] Li Z., Deng Y., Shen B., Liu L., Hu W.: 'Synthesis, characterization and microwave properties of Ni–Co–P hollow spheres', *J. Alloys Compd.*, 2010, **491**, pp. 406–410

[19] Joseyphus R.J., Kodama D., Matsumoto T., Sato Y., Jeyadevan B., Tohji K.: 'Role of polyol in the synthesis of Fe particles', *J. Magn. Magn. Mater.*, 2007, **310**, pp. 2393–2395

[20] Fievet F., Fievet-Vincent F., Lagier J.P., Dumont B., Figlarz M.: 'Controlled nucleation and growth of micrometre-size copper particles prepared by the polyol process', *J. Mater. Chem.*, 1993, **3**, pp. 627–632

[21] Balke B., Fecher G.H., Felser C.: 'Structural and magnetic properties of $Co_2FeAl_{1-x}Si_x$', *Appl. Phys. Lett.*, 2007, **90**, pp. 242503–242505

[22] Wurmehl S., Fecher G.H., Kroth K., *ET AL.*: 'Electronic structure and spectroscopy of the quaternary Heusler alloy $Co_2Cr_{1-x}Fe_xAl$', *J. Phys. D, Appl. Phys.*, 2006, **39**, pp. 803–815

[23] Hirohata A., Kikuchi M., Tezuka N., *ET AL.*: 'Heusler alloy/semiconductor hybrid structures', *Curr. Opin. Solid State Mater. Sci.*, 2006, **10**, pp. 93–107

[24] Kodama D., Shinoda K., Sato K., *ET AL.*: 'Chemical synthesis of sub-micrometer-to nanometer-sized magnetic FeCo dice', *Adv. Mater.*, 2006, **18**, pp. 3154–3159

[25] Nguyen Q., Chinnasamy C.N., Yoon S.D.: 'Functionalization of FeCo alloy nanoparticles with highly dielectric amorphous oxide coatings', *J. Appl. Phys.*, 2008, **103**, pp. 07D532–07D534

[26] Zachary J.H., Kyler J.C., Everett E.C.: 'Synthesis of high magnetization FeCo alloys prepared by a modified polyol process', *J. Appl. Phys.*, 2011, **109**, pp. 07B514–07B516

doi: 10.1049/mnl.2012.0905